

Synthesis of composite Mg–Ni–Ca metal hydride by mechanical alloying

Eun Young Lee*, Kyung Sub Jung, Kyung Sub Lee

Division of Advanced Materials Science and Engineering, Hanyang University, 133-791 Seoul, South Korea

Received 23 September 2006; received in revised form 21 December 2006; accepted 21 December 2006

Available online 8 January 2007

Abstract

Amorphous and composite Mg–Ni–Ca metal hydrides were synthesized by mechanical alloying. $(\text{Mg}_{0.5}\text{Ca}_{0.5})\text{Ni}_2$ yielded the composite of Mg_2Ni and CaNi_5 , while $\text{MgNi}_{0.95}\text{Ca}_{0.05}$ produced the amorphous phase. The initial discharge capacities of the amorphous $\text{MgNi}_{0.95}\text{Ca}_{0.05}$ alloy and the composite $(\text{Mg}_{0.5}\text{Ca}_{0.5})\text{Ni}_2$ alloy were 460 and 210 mAh/g, respectively. After 20 cycles, the amorphous electrode retained 11% of the initial discharge capacity while the composite electrode maintained 64% of the initial discharge capacity. After 10 cycles, the XPS analysis showed that Mg spectra of the amorphous $\text{MgNi}_{0.95}\text{Ca}_{0.05}$ alloy was shifted to a lower binding energy because Mg reacted with OH^- of the electrolyte. However, Mg spectra of the composite $(\text{Mg}_{0.5}\text{Ca}_{0.5})\text{Ni}_2$ alloy showed that the binding energy did not change during the cycle test. These results indicate that the amorphous phase had the highest discharge capacity and the composite formation improved the cyclic stability.
© 2007 Elsevier B.V. All rights reserved.

Keywords: Metal hydride; Calcium; Amorphous; Composite; Electrode properties

1. Introduction

Mg–Ni based metal hydride is among the most promising material for Ni–MH batteries due to its large theoretical discharge capacity of Mg_2NiH_4 (999 mAh/g), low cost, light weight and environmental compatibility. However, Mg–Ni based metal hydride has some shortcomings such as low electrochemical discharge capacity at room temperature and degradation in the alkaline electrolyte. To overcome these problems, the manufacture of the amorphous phase and synthesis of a composite alloy have been widely studied [1–4]. Ruggery et al. [5] reported that mechanically alloyed amorphous Mg–Ni had an initial discharge capacity of 500 mAh/g at room temperature. The amorphous materials improve their discharge capacity because of many defects, such as dislocations and grain boundaries that affect the diffusivity and solubility of hydrogen [6,7].

Composite hydride materials composed of two or more hydrogen storage alloys or intermetallic compounds have been researched as a class of electrode materials [8,9]. The major component generally acts as the main hydrogen storage medium having good discharge capacity. The minor component is char-

acterized by a surface activator to enhance cycle stability and kinetics of hydrogenation, as well as to ease the initial activation of the major component. Han et al. [10] synthesized composite metal hydride of Mg_2Ni and TiNi phases by ball milling and sintering. The cyclic stability of the composite metal hydride was greatly enhanced by hydrogen diffusion through the interface between Mg_2Ni and TiNi.

The Mg–Ni–Ca system was selected in the present work to synthesize amorphous and composite alloys. Calcium was added to Mg–Ni alloys as partial substitution of Mg and Ni. It was expected to synthesize a composite composed of Mg–Ni and Ca–Ni intermetallic compounds. The Ca–Ni intermetallic compounds are CaNi_2 , CaNi_3 , Ca_2Ni_7 and CaNi_5 . Among them, CaNi_5 has been of interest because its surface has good activation property [11].

In this study, composite and amorphous alloys were synthesized by mechanical alloying of elemental powders of Mg, Ni and Ca. Structural characterization was carried out before and after cycle tests and the electrochemical properties were compared with ball-milled Mg_2Ni under the same conditions.

2. Experimental details

Mg–Ni–Ca alloys were synthesized by mechanical alloying with SPEX-8000 for 7 h. The charging compositions are listed in Table 1. The starting

* Corresponding author. Fax: +82 2 2281 4914.
E-mail address: quf100@hanyang.ac.kr (E.Y. Lee).

Table 1
Composition of alloys produced by ball milling (in mol fraction)

Designation	Element		
	Mg	Ni	Ca
MgNi	1	1	0
MgNi _{0.95} Ca _{0.05}	1	0.95	0.05
(Mg _{0.5} Ca _{0.5})Ni ₂	0.5	2	0.5

materials consisting of Mg (Sigma–Aldrich Co., 99.8%, $\leq 30 \mu\text{m}$), Ni (Kosundo Chemical Co., 99.9%, $\leq 63 \mu\text{m}$) and Ca (Johnson Matthey Co., 99.5%, granule) were charged to a Cr–Ni steel vial with two 1/2-in. and four 1/4-in. diameter Cr–Ni steel balls. The ball to powder weight ratio was 10:1. The powders were handled and mechanically alloyed under Ar atmosphere.

The structures of the ball milled powders were examined by X-ray diffraction (XRD, Rigaku D-MAX2500) with Cu K α radiation and microstructure studies were performed by scanning electron microscopy (SEM, JEOL JSM-6340F) with Energy-Dispersive X-ray Spectrometer (EDX).

For electrochemical examination, the synthesized powders were cold pressed and 10 mm diameter pellet-type electrodes were made, under 5.0 t/cm^2 . The electrochemical examination was conducted in a half-cell with three electrodes which consisted of the metal hydride as the working electrode, a Hg/HgO reference electrode, and a platinum counter electrode in 6 M KOH·1 M LiOH electrolyte. The cycle tests were performed at room temperature using an automatic galvanostatic charge–discharge unit (Maccor series 4000) at a current discharge density of 10 mA/g. The discharge cut-off potential was set at -0.6 V with respect to the reference electrode.

After the cycle tests, the electrodes were washed in distilled water and dried overnight at 60°C . The phase changes of the electrodes before and after cycle testing were examined by XRD. To investigate the changes of the binding energy for elemental Mg on the alloy surface of each electrode, X-ray Photoelectron Spectroscopy (XPS, VG ESCALAB-220I) was carried out using AlK α radiation.

3. Results and discussion

3.1. Structural analysis

X-ray diffraction patterns of the synthesized powders of MgNi, MgNi_{0.95}Ca_{0.05} and (Mg_{0.5}Ca_{0.5})Ni₂ compositions are shown in Fig. 1. The MgNi powder ball-milled for 7 h produced the crystalline Mg₂Ni with unreactive Ni. MgNi_{0.95}Ca_{0.05} had an amorphous phase, while (Mg_{0.5}Ca_{0.5})Ni₂ yielded a composite of Mg₂Ni and CaNi₅. The ball-milled composite did not match stoichiometrically, which the remaining Ca_{0.25} presumably contributed to form amorphous. The substitution of Ca for Ni in the MgNi accelerated the formation of amorphous because the amorphous MgNi had been previously reported to be formed by milling the elemental powders of Mg and Ni for 10 h [12]. The composite phase was synthesized upon the substitution of 50 at% Ca for Mg in MgNi₂ by ball milling alone. Both the synthesized Mg₂Ni and the amorphous MgNi_{0.95}Ca_{0.05} had remaining Ni. The remaining elemental Ni would have a catalytic effect and act as a current collector in electrochemical reactions.

Fig. 2 shows the SEM micrographs of the synthesized alloys and EDX line mapping of Mg and Ni in the composite alloy. The average particle sizes of the ball milled Mg₂Ni and the amorphous MgNi_{0.95}Ca_{0.05} were about 10 and $2 \mu\text{m}$, respec-

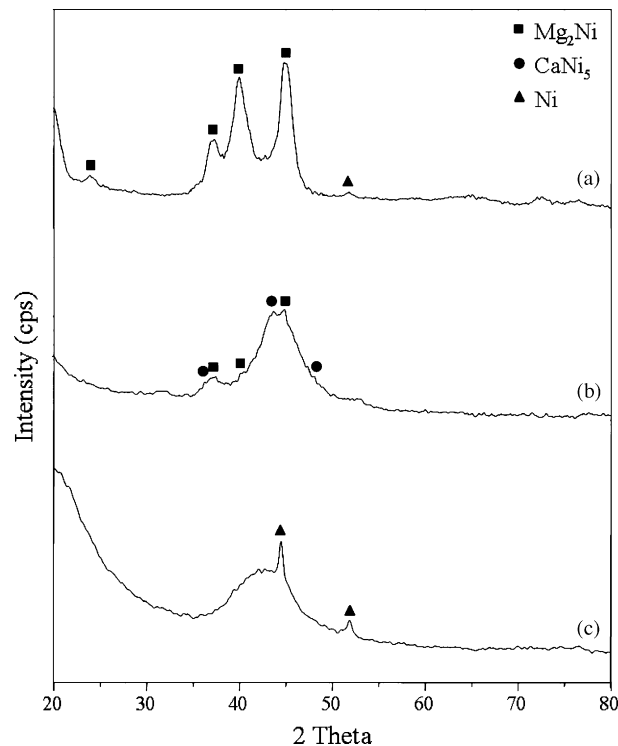


Fig. 1. XRD data of the ball-milled Mg₂Ni, amorphous and composite alloys: (a) Mg₂Ni; (b) (Mg_{0.5}Ca_{0.5})Ni₂; (c) MgNi_{0.95}Ca_{0.05}.

tively. In the case of the composite alloy, the CaNi₅ particles with average diameter size of about 24 nm were attached to the surface of the Mg₂Ni particles the average diameter of which were of about $1 \mu\text{m}$. The particle sizes of both Mg₂Ni and CaNi₅ were calculated by Scherrer's formula from the XRD data [13]. In order to identify the distribution of Mg and Ca in the Mg₂Ni and CaNi₅ phase, EDX line mapping was performed. Bigger particles were Mg₂Ni and nano particles of CaNi₅ were distributed on the surface of Mg₂Ni particles.

3.2. Electrochemical properties and phase transformation after cycle test

Fig. 3 shows the discharge capacity of the ball-milled Mg₂Ni, amorphous MgNi_{0.95}Ca_{0.05} and composite electrodes in 6 M KOH·1 M LiOH electrolyte. All of the electrodes revealed the maximum discharge capacities at the first cycle. Among the electrodes, the amorphous MgNi_{0.95}Ca_{0.05} electrode had the highest initial discharge capacity of 460 mAh/g, which was much higher than that of the ball-milled Mg₂Ni. This indicated that the high electrochemical activity of the amorphous alloys was due to easy hydrogen diffusion in the amorphous matrix and the catalytic effects of the remaining metallic Ni [14]. However, the degradation rate of the amorphous alloy electrode was the highest. It was able to maintain 11% of the initial discharge capacity after 20 cycles. For the composite electrode, the initial discharge capacity was lower than that of the ball-milled Mg₂Ni of 288 mAh/g, but its capacity retained 64% of the initial capac-

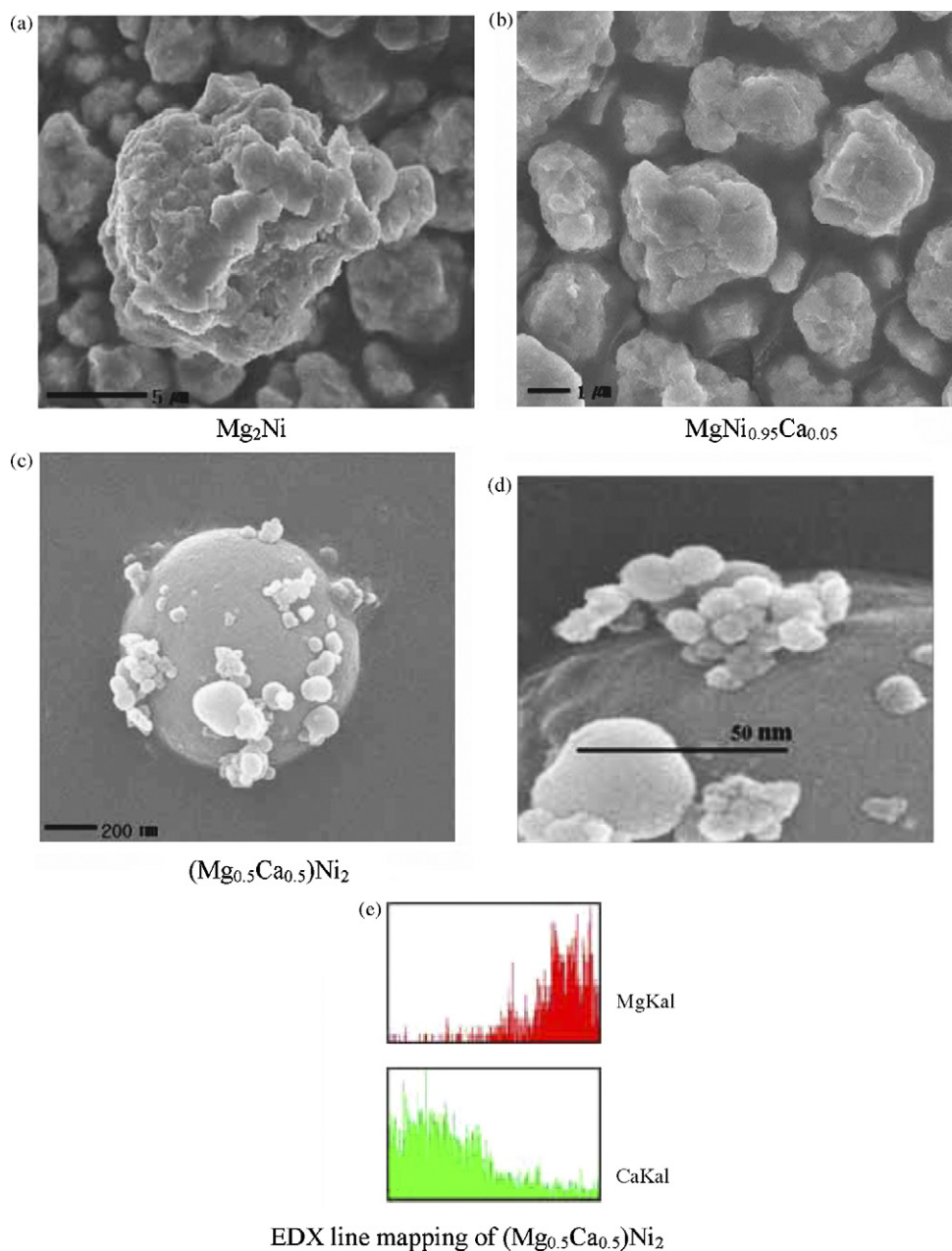


Fig. 2. SEM micrographs of the synthesized alloys and EDX line mapping of composite.

ity of 207 mAh/g after 20 cycles. Until 10 cycles, the discharge capacity of composite alloy electrode markedly decreased to 30% of the initial capacity and after then showed the best cyclic stability.

The XRD patterns of electrodes after 10 cycle tests are shown in Fig. 4. The $\text{Mg}(\text{OH})_2$ peak appeared due to oxidation of Mg on the surfaces of the Mg_2Ni and the amorphous $\text{MgNi}_{0.95}\text{Ca}_{0.05}$ electrodes. The formation of the oxide was caused by dissolution or precipitation of constituent elements in the electrolyte during the cycle test [15]. The composite alloy electrode was not oxidized but transformed to the amorphous phase due to the so-called hydrogen-induced amorphization (HIA) phenomenon. K. Aoki and T. Masumoto reported that amorphizing intermetallics

with AB-, AB₂-, A₂B-type composition occurred during the hydrogen charging [16].

The XPS data spectra of the amorphous and composite electrodes agree with the XRD data. The peak of the amorphous $\text{MgNi}_{0.95}\text{Ca}_{0.05}$ alloy shifted to a higher binding energy with cycle numbers (Fig. 5(a)). Fuggle et al. [17] suggested that the binding energy of the Mg 2p increased about 2–3 eV when Mg was reacted with oxygen. Thus, it was thought that the shift of the XPS peak of the amorphous alloy was generated by the formation of a $\text{Mg}(\text{OH})_2$ layer. Mg 2p spectra of the composite electrode changed after 2 cycles, and remained constant for further cycles (Fig. 5(b)). The change of the XPS peak of the composite electrode after 2 cycles may be caused

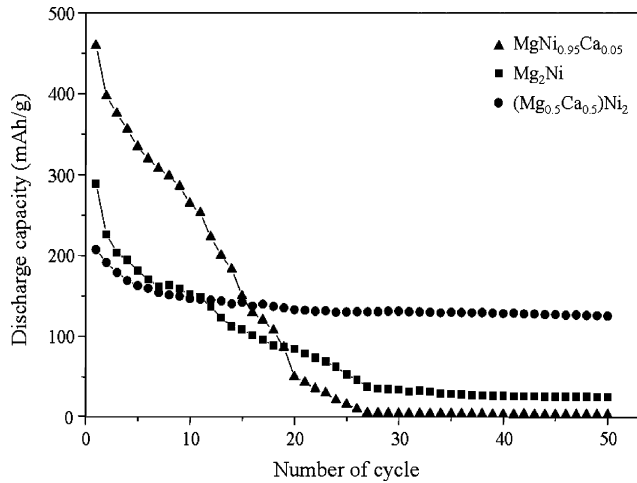


Fig. 3. Cycle test data of the ball-milled Mg₂Ni, amorphous and composite alloys.

by phase transformation to the amorphous. The atomic binding of Mg at the amorphous phase is known to be lower than of the crystalline phase [18]. Although the composite electrode transformed to the amorphous phase, it enhanced cycle stability different from ball-milled amorphous alloy. From Ca spectra in XPS data with number of cycles (not shown), peaks of Ca 2p shifted to higher binding energy, which means Ca was oxidized during cycle tests. Therefore, CaNi₅ on the surface of Mg₂Ni contributed to prevent oxidation of Mg in MgNi because Ca has lower potential than Mg. The amorphous electrode was rapidly degraded by oxidation of dissolved Mg. However, the composite electrode showed the relatively good cyclic stability because oxidation layer of Mg was not readily formed although the composite electrode changed to amorphous phase. Moreover,

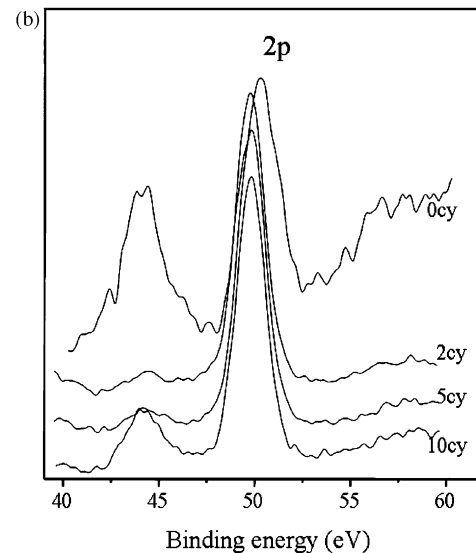
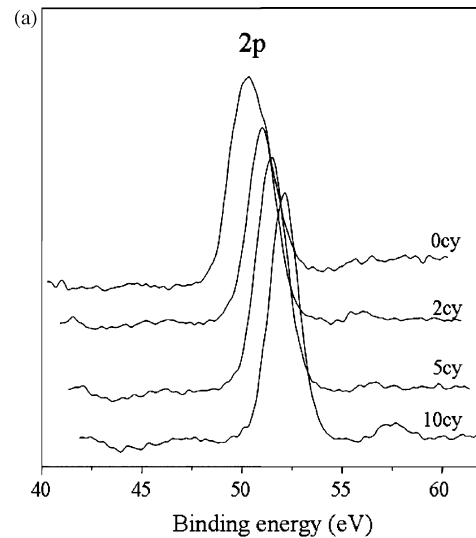


Fig. 5. XPS spectra for Mg 2p with cycle number: (a) amorphous electrodes; (b) composite electrodes.

CaNi₅ may have contributed to cycle life with its stability in the electrolyte.

4. Conclusions

The amorphous and composite of Mg₂Ni and CaNi₅ alloys were synthesized under the same milling condition but different composition. The composite metal hydride was directly made from Mg, Ni and Ca elemental powders. The amorphous phase of the metal hydride contributed to the improved discharge capacity due to the high diffusivity of hydrogen and catalytic effect of many defects. On the other hand, the degradation rate of the amorphous alloy was increased by dissolution of the active materials and oxidation of Mg on the electrode surface. The composite electrode had lower maximum discharge capacity, but enhanced cyclic stability compared to the Mg₂Ni electrode. The cyclic stability was enhanced by preventing formation of the passive Mg(OH)₂ layer.

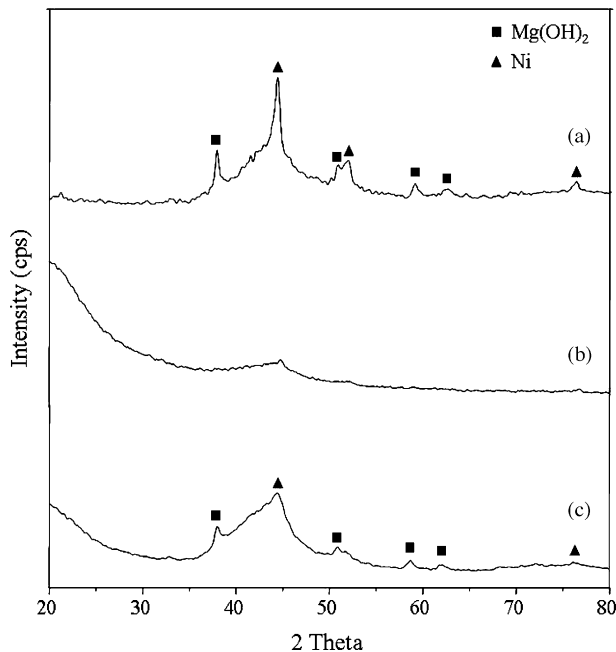


Fig. 4. XRD patterns after 10 cycle tests: (a) Mg₂Ni; (b) (Mg_{0.5}Ca_{0.5})Ni₂; (c) MgNi_{0.95}Ca_{0.05}.

References

- [1] S.C. Han, P.S. Lee, J.Y. Lee, A. Zuttel, L. Schlapbach, *J. Alloys Compd.* 306 (2000) 219.
- [2] C. Rongeat, L. Loue, *J. Alloys Compd.* 404–406 (2005) 679.
- [3] S.M. Han, Z. Zhang, M.S. Zhao, Y.Z. Zheng, *Int. J. Hydrogen Energy* 31 (2006) 563.
- [4] S. Srivastava, O.N. Srivastava, *J. Alloys Compd.* 290 (1999) 250.
- [5] S. Ruggeri, C. Lenain, L. Roue, H. Alamdari, G. Liang, J. Huot, R. Schulz, *Mater. Sci. Forum* 11 (2001) 63.
- [6] S. Orimo, K. Ikeda, H. Fujii, Y. Kitamo, K. Yamamoto, *Acta Mater.* 45 (1997) 2271.
- [7] T. Spassov, U. Koster, *J. Alloys Compd.* 287 (1999) 243.
- [8] S.R. Ovshinsky, M.A. Fetcenko, *Appl. Phys. A* 72 (2001) 239.
- [9] J. Huot, J.F. Pelletier, L.B. Lurio, M. Sutton, R. Schulz, *J. Alloys Compd.* 248 (2003) 319.
- [10] S.S. Han, N.H. Goo, K.S. Lee, *J. Alloys Compd.* 360 (2003) 243.
- [11] H. Imamura, Y. Noda, Y. Sakata, S. Tsuchiya, *J. Alloys Compd.* 323–324 (2001) 601.
- [12] S. Ruggeri, L. Roue, G. Liang, J. Huot, R. Schelz, *J. Alloys Compd.* 339 (2002) 195.
- [13] B.D. Cullity, S.R. Stock, *Elements of X-ray Diffraction*, 3rd ed., Prentice-Hall, 2001, p. 170.
- [14] N.H. Goo, K.S. Lee, *Int. J. Hydrogen Energy* 27 (2002) 433.
- [15] J.H. Jung, H.H. Lee, D.M. Kim, K.J. Jang, J.Y. Lee, *J. Alloys Compd.* 266 (1998) 266.
- [16] K. Aoki, T. Masumoto, *J. Alloys Compd.* 231 (1995) 20.
- [17] J.C. Fuggle, L.M. Watson, D.J. Fabian, S. Affrossman, *Met. Phys.* 5 (1975) 375.
- [18] H.Y. Lee, N.H. Goo, W.T. Jeong, K.S. Lee, *J. Alloys Compd.* 313 (2000) 258.